GEOPHYSICS, VOL. 71, NO. 6 (NOVEMBER-DECEMBER 2006); P. F173–F183, 13 FIGS., 2 TABLES.
10.1190/1.2358494

Gassmann's fluid substitution and shear modulus variability in carbonates at laboratory seismic and ultrasonic frequencies

Ludmila Adam[1], Michael Batzle[1], and Ivar Brevik[2]

ABSTRACT

Carbonates have become important targets for rock property research in recent years because they represent many of the major oil and gas reservoirs in the world. Some are undergoing enhanced oil recovery. Most laboratory studies to understand fluid and pressure effects on reservoir rocks have been performed on sandstones, but applying relations developed for sandstones to carbonates is problematic, at best. We measure in the laboratory nine carbonate samples from the same reservoir at seismic (3–3000 Hz) and ultrasonic (0.8 MHz) frequencies. Samples are measured dry (humidified) and saturated with liquid butane and brine. Our carbonate samples showed typical changes in moduli as a function of porosity and fluid saturation. However, we explore the applicability of Gassmann's theory on limestone and dolomite rocks in the context of shear- and bulk-modulus dispersion and Gassmann's theory assumptions. For our carbonate set at high differential pressures and seismic frequencies, the bulk modulus of rocks with high-aspect-ratio pores and dolomite mineralogy is predicted by Gassmann's relation. We also explore in detail some of the assumptions of Gassmann's relation, especially rock-frame sensitivity to fluid saturation. Our carbonate samples show rock shear-modulus change from dry to brine saturation conditions, and we investigate several rock-fluid mechanisms responsible for this change. To our knowledge, these are the first controlled laboratory experiments on carbonates in the seismic frequency range.

INTRODUCTION

An important area of research for carbonate rocks is the fluid substitution effect on elastic moduli and velocities. One of the widely used relations to estimate the effect of fluids on bulk modulus is Gassmann's fluid substitution theory (Gassmann, 1951), which we examine in the following section. Laboratory measurements on carbonates have been performed at ultrasonic frequencies (~0.8 MHz) to estimate the validity of Gassmann's equations for limestones and dolomites (Wang et al., 1991; Marion and Jizba, 1997; Wang, 2000; Baechle et al., 2005; Røgen et al., 2005). In most cases Gassmann's predictions underestimate the observed ultrasonic velocities for either oil- or brine-saturated samples, although for some samples, Gassmann's theory overestimates the measured velocities (Wang, 2000; Baechle et al., 2005; Røgen et al., 2005).

Presently, the applicability of Gassmann's equation to carbonate rocks is unresolved. With our work, we hope to make inferences about the uncertainties and interpretation on the applicability of Gassmann's equation. Our work focuses on understanding the applicability of Gassmann's fluid-substitution theory at seismic and ultrasonic frequencies. We also analyze the validity of some of the assumptions for Gassmann's theory, especially rock-frame sensitivity to fluids. Our carbonate samples consist of different fabrics, mineralogies, porosities, and permeabilities; still, we must be careful in generalizing our results to all carbonate reservoirs.

First, we present Gassmann's theory and its assumptions. Second, we describe the laboratory acquisition, processing, and data uncertainty analysis at seismic and ultrasonic frequencies. Then, we introduce shear modulus variability with fluid substitution and the possible mechanisms that could explain these changes. Finally, we compare our measured bulk modulus to Gassmann's predictions for these carbonate rocks.

GASSMANN'S EQUATION

Gassmann's fluid-substitution relation is commonly applied to predict the bulk modulus for rocks saturated with different fluids:

Manuscript received by the Editor April 18, 2006; revised manuscript received June 29, 2006; published online October 26, 2006.
[1]Colorado School of Mines, Center for Rock Abuse, Department of Geophysics, 1500 Illinois Street, Golden, Colorado 80401. E-mail: ladam@mines.edu; mbatzle@mines.edu.
[2]Statoil Research Centre, Postuttak, N7500 Trondheim, Norway. E-mail: ivb@statoil.com.

$$K_{sat} = K_{dry} + \frac{\left(1 - \frac{K_{dry}}{K_{min}}\right)^2}{\frac{\phi}{K_{fl}} + \frac{1-\phi}{K_{min}} - \frac{K_{dry}}{K_{min}^2}}. \quad (1)$$

Gassmann's equation 1 estimates the saturated bulk modulus (K_{sat}) through the bulk modulus of the forming minerals (K_{min}), the bulk modulus of the frame or dry rock (K_{dry}), the bulk modulus of the fluid (K_{fl}), and the rock porosity (ϕ) (Gassmann, 1951). Note that in Gassmann's relation, the considered property of the fluid in the rock is only the fluid bulk modulus.

Gassmann's derivation is based on the following assumptions for a porous system:

1) Pore pressure is in equilibrium between pores. This can be achieved at very low frequencies, usually at seismic frequencies or lower, where the fluid has enough time to reach relaxation or equilibrium. However, the relaxation time depends also on fluid viscosity and density, and rock permeability.
2) The porous frame consists of a single solid material (monomineralic).
3) Pores are in flow communication and are homogeneously fully filled with a nonviscous fluid.
4) The system is closed (undrained).
5) The pore fluid does not chemically influence the solid frame.

Although implied, a constant rock shear modulus from dry to any fluid-type saturation is not an assumption but an outcome of Gassmann's theory (Berryman, 1999).

The beauty of equation 1 is its simplicity as well as the fact that the variables have physical significance and are usually well constrained or can be directly measured. Other fluid substitution theories require the knowledge of such factors as the symmetry of the rock, the geometry of the inclusions, and the crack density among others. For example, in the low-frequency limit where no pore-pressure gradients exist, Brown and Korringa (1975) relate the anisotropic rock effective elastic compliance tensor to the same rock filled with fluid; for an isotropic and monomineralic rock, their relations reduce to Gassmann's equation. For this fluid-substitution theory, knowledge of the anisotropic symmetry and pore-space compressibility are required. Other fluid-substitution theories mostly assume isolated inclusions and their geometries in the derivation of the equations. Isolated cavities should then also be isolated with respect to fluid flow (presence of pore-pressure gradients). Therefore, theories that assume isolated inclusions (Kuster and Toksoz, 1974; O'Connell and Budiansky, 1974; Hudson, 1981) may be more applicable to the high-frequency range and require knowledge of parameters related to pore space.

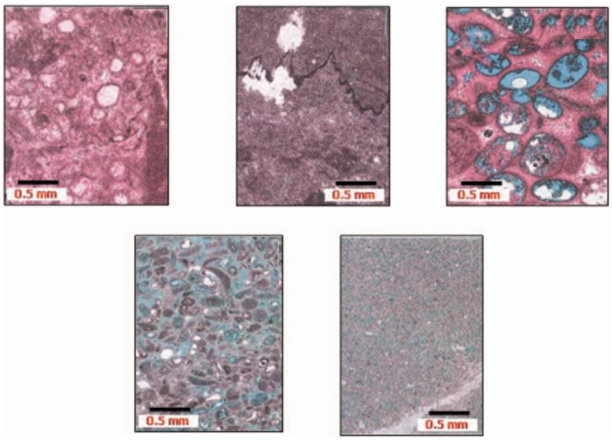

Figure 1. Thin sections for some of the carbonate samples. Pink represents calcite; gray, dolomite; white, anhydrite; and blue, pore space.

CARBONATE SAMPLES

Our carbonates are from two wells in a single reservoir with depths between 2915 and 3180 m below sea level. The reservoir has lagoon, ramp, and shoal depositional environments. These different depositional systems create different textures, porosities, and permeabilities (Figure 1). Some reservoir regions have been dolomitized. Dolomitization is evident from high porosity and high permeability because dissolved grains or fossils become pore space, increasing the connectivity between pores, thus increasing permeability. The reservoir is not fractured and has few clay minerals but does have minor anhydrite. The available samples comprise nine carbonates with varying porosity (5%–35%), permeability (0.03–432 md), mineralogy (dolomite and limestone), and texture. The samples are either almost pure calcite or dolomite (95% total volume) with less than 4% clays and 5% anhydrite of total volume. Samples wialtth large anisotropy or vuggy pores are avoided. Table 1 summarizes the petrological data for our samples. Porosity and permeability are measured using standard helium porosimetry and air-permeability equipment at atmospheric pressure. Permeability values are corrected for Klinkenberg gas slippage. The samples are cylindrical, 3.75 cm in diameter and 3.75–5 cm in length.

Velocity and elastic modulus data are acquired at nine pressure points. Confining pressure varies from 3.5 to 34.5 MPa, while pore pressure is held constant at 3.5 MPa, thus reaching a maximum differential pressure of 31 MPa. The low-frequency system in the laboratory is pressurized with nitrogen gas, but for safety reasons the system is not able to reach the reservoir differential pressure (34.5 MPa). Samples are measured dry, under butane (C_4H_{10}), and under brine (200,000 ppm NaCl) saturations. Butane, at 3.5 MPa, is in liquid state. Samples are measured with some amount of moisture because even less than 1% of water can reduce the bulk and shear moduli significantly (Clark et al., 1984). Because samples show sensitivity to water, several are kept in a high-humidity chamber to provide an initial brine saturation (less than 1%). Samples *A*, *C*, *E*, *F*, and *G* are humidified previous to measurements; thus, dry for these samples means humidified. Samples *B*, *D*, *H*, and *I* are measured at room conditions (30% humidity). Samples are coated with a thin, impermeable polyimide film (Kapton), over which strain gauges are glued to measure rock deformations at seismic frequencies. This film keeps the moisture inside the rock and prevents nitrogen diffusion.

DATA EXAMPLE: ACQUISITION AND PROCESSING

Samples are measured at low (seismic: 3–3000 Hz) and ultrasonic (~0.8 MHz) frequencies , although sample *G* is measured at ultrasonic frequencies only. Seismic frequency moduli and velocities are derived from the stress-strain method (Spencer, 1981; Batzle et

al., 2006). Measured strains on the rock and a calibrating material (aluminum) are converted into Young's modulus and Poisson's ratio, and from these we get bulk and shear moduli. Batzle et al. (2006) give a detailed description of the apparatus and the estimation of elastic moduli from measured strains. In the stress-strain experiment, we directly estimate the bulk and shear moduli. Thus, our moduli estimates are independent of the rock density. As we will see, for ultrasonic data the rock density is needed to estimate the bulk and shear moduli.

For ultrasonic data, we measure the time a wave takes to propagate from the top of the sample to the bottom (Birch, 1960). The velocity, either P- or S-wave, is estimated by $V = (L - \delta L)/(T_m - T_0)$, where L is the sample length measured at atmospheric pressure, δL is the change in sample length from pressurization, T_m is the measured traveltime, and T_0 is a time correction. The value δL is ignored because the change in length, which we can estimate from the low-frequency experiment, is very small. The value T_0, the traveltime through the aluminum material between the ultrasonic transducer and the sample, is known and constant for all measured samples. Therefore, we can rewrite the velocity as $V = L/T$, where T is the corrected traveltime. Assuming isotropy, the measured velocities and densities are then used to derive the shear and bulk moduli.

As an example of the estimated bulk modulus over the entire frequency range, we show results for sample *H* in Figure 2. The computation of the error bars and the linear fit are discussed later in this section. Observe that the rock bulk modulus increases with saturating fluid. However, the change in rock bulk modulus from dry to butane saturated is small compared to when the rock is saturated with brine. This is because butane has a lower fluid bulk modulus than brine. Figure 2 also shows bulk-modulus dispersion (higher frequencies have a larger modulus). Several theories exist to explain the nature of this dispersion. A primary cause for dispersion can be pore-pressure disequilibrium caused by nonzero pore-pressure gradients. This unrelaxed pressure is described by several mechanisms: grain-fluid inertial and viscous coupling (Biot, 1956), patchy saturation (White, 1975; Dutta and Ode, 1979), and squirt or local fluid flow (Mavko and Jizba, 1991), among others. Our goal here is not to decide which frequency-dependent modulus or velocity theories are causing the dispersion. We do want to point out differences in modulus estimates as a result of the dispersion from seismic to ultrasonic frequencies. As previously mentioned, Gassmann's theory is for the low-frequency limit, meaning that this theory may not be suitable to predict ultrasonic data because of possible dispersion in the elastic moduli and velocities. Wang (1997), Marion and Jizba (1997), Baechle et al. (2005), and Røgen et al. (2005) have shown how, in most cases, Gassmann's theory underpredicts ultrasonic frequency measurements. Pore pressure can equilibrate if there is enough time for the fluids to relax. This means there is a characteristic frequency f_c of the rock perturbation. For measurements acquired at a frequency less than f_c, the pore pressure has reached equilibrium; while for higher frequencies than f_c, pore fluids are not equilibrated, producing higher values for modulus and velocity.

Differential pressure also controls the modulus dispersion of a rock. At low differential pressures where compliant pores or cracks are open, pore-pressure disequilibrium is more likely to occur. Wang (2000) shows, in a compilation of ultrasonic laboratory data of carbonate samples, that Gassmann's theory substantially (up to 30%) underpredicts the measured velocities at low differential pressures. At high differential pressures, compliant pores close, and Gassmann's theory predicts the measured data within 10%.

Carbonates are heterogeneous, and vugs or moldic structures can have comparable length to the ultrasonic wavelength (0.5 cm for a wave at 0.8 MHz and with a velocity of 4500 m/s). Some of our samples showed inclusions of different densities or voids with dimensions on the order of ultrasonic wavelengths. Therefore, scattering of ultrasonic waves is possible in carbonate samples, especially in dry rocks where the density contrast between voids and the matrix is large. When scattered, the wave loses energy to multiple reflections from grains, mostly resulting in lower moduli and velocities at higher frequencies. The larger modulus contrast will be for air-grain and butane-grain interfaces.

Poisson's ratio: A correction

Samples *B*, *F*, and *I* show higher values of Poisson's ratio at low frequency than expected in carbonates. Rock heterogeneity is probably not the cause because placing the strain gauges on large heterogeneities (visible to the eye) on measured core plugs is avoided. The

Table 1. Petrological data for the carbonate set. Mineralogy was obtained from X-ray (XRD) diffraction analysis and is reported in percent per volume (samples E, G, and H had no XRD analysis). Mineral bulk modulus is computed using Voigt-Reuss-Hill average. Texture follows modified Dunham's carbonate classification (Moore, 2001): mud = mustone, wacke = wackestone, pack = packstone, grain = grainstone, and bound = boundstone.

Samples	A	B	C	D	E	F	G	H	I
Porosity (%)	1.6	4.6	21.0	24.9	28.5	34	23.6	29.6	34.7
Permeability (md)	0.03	0.03	5.50	1.20	0.43	0.31	25.00	103.00	432.00
Grain density (g/cm^3)	2.73	2.84	2.70	2.71	2.70	2.69	2.84	2.80	2.86
Calcite (%)	83.0	0.7	76.0	99.6	—	97.0	—	—	0.4
Dolomite (%)	11.0	97.0	21.0	0.0	—	0.0	—	—	93.0
Anhydrite (%)	0.5	0.5	0.0	0.0	—	0.7	—	—	4.9
Phyllosilicates (%)	3.4	0.8	2.4	0.0	—	2.3	—	—	1.1
Quartz (%)	0.6	0.6	1.2	0.4	—	0.2	—	—	0.8
K-feldspar (%)	2.0	0.0	0.0	0.0	—	0.0	—	—	0.0
Mineral bulk modulus (GPa)	70.70	78.96	71.59	71.26	71.59	70.35	85.00	78.96	77.67
Texture	Wacke	Mud	Grain	Grain	Grain	Bound	Pack	Wacke	Mud

observed larger deformations of the sample in the horizontal direction probably result from end effects in our stress-strain system. This large deformation or bulging can result from the combination of intrinsically large Poisson's ratios in carbonates (>0.25) and short samples (our sample length is close to its diameter). This bulging has been confirmed with preliminary finite-element modeling at our laboratory. Poisson's ratio depends on V_P/V_S; but because the dispersion in V_P and V_S are similar for our samples, the resulting dispersion in Poisson's ratio is negligible, making it possible to correct the low-frequency data with the estimates we obtain from ultrasonic data. Domenico (1984), Anselmetti and Eberli (1993), Mavko et al. (1998), Assefa et al. (2003), and Han (2004) measured carbonate samples ultrasonically and derived empirical relations for V_P and V_S. We use their relations to compute Poisson's ratio for water/brine-saturated carbonates and compare their values to our samples' Poisson's ratio measured at ultrasonic frequencies (Figure 3). Agreement between the modeled Poisson's ratio and our measurements lets us use the ultrasonic values to correct the Poisson low-frequency data. The correction consists of multiplying the seismic-frequency Poisson's ratio by a factor less than one. This factor is obtained from the ratio of the ultrasonic and the biased seismic-frequency Poisson's ratios.

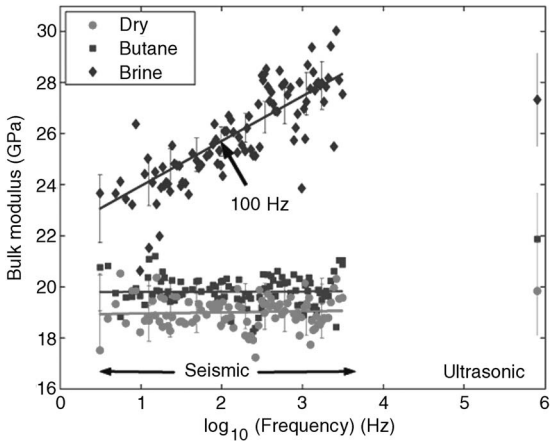

Figure 2. Seismic- and ultrasonic-frequency bulk-modulus least-squares estimates (solid lines) and measured data for sample *H* at 31 MPa. Observe the modulus dispersion for different fluids. Error bars are two standard deviations of the estimated bulk modulus.

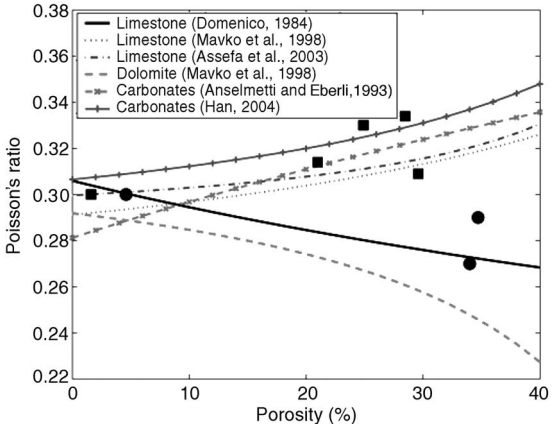

Figure 3. Modeled Poisson's ratio from empirical relations from ultrasonic data for carbonate rocks saturated with water/brine. Squares and circles are the Poisson's ratios obtained from our measurements at ultrasonic frequencies. Our values of Poisson's ratio agree with the empirical equations. Therefore, we use the ultrasonic Poisson's value to correct the low-frequency data for our samples (*B*, *F*, and *I*) represented by circles.

Uncertainty analysis

Our data set consists of Poisson's ratio and Young's modulus as a function of frequency and differential pressure (seismic frequency) and traveltime as a function of differential pressure (ultrasonic frequency). We assume that Poisson's ratio and Young's modulus relation to the logarithm base 10 of frequency is linear, whereas the traveltime with differential pressure follows a second order polynomial (true models). We also assume that the error between our data and these true models is random, Gaussianly distributed, and with zero mean. Our core analysis is performed under the assumption that all requirements for Gassmann's theory applicability are satisfied. If our samples and experimental setup violate one (or more) of the assumptions of Gassmann's theory, we introduce a bias (systematic error) in our estimates, and we will give an interpretation to why some results on the samples do not obey Gassmann's assumptions.

Stress-strain methodology

In Figure 4, we plot data for the stress-strain experiment (E and ν) showing a linear trend with $\log_{10}$ of frequency. We fit a straight line to our data and estimate the variance of our random error. We use the variance of the random error to compute the error of estimates of Young's modulus and Poisson's ratio, and later propagate this error into the estimates of bulk and shear moduli. Young's modulus of aluminum equals 70 GPa (needed to compute the rock Young's modulus), and we assume this value is error free for the uncertainty analysis. On average, our estimates of the standard deviation of the estimated bulk modulus is 1.2 GPa and that of the shear modulus is 0.3 GPa for seismic frequencies.

Ultrasonic pulse propagation

In addition to low-frequency measurements, we have traveltimes at 0.8 MHz versus differential pressure. Traveltime decreases with increasing differential pressure (higher velocity). Figure 5 shows

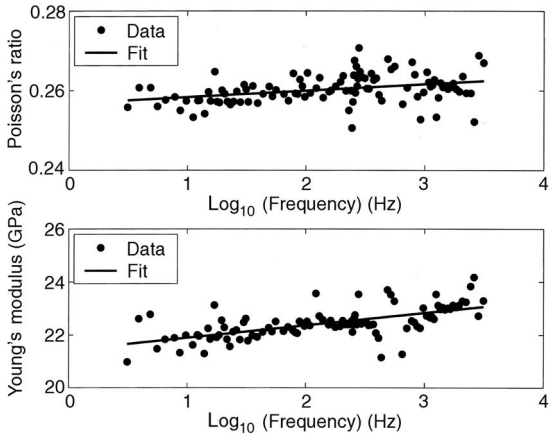

Figure 4. Error analysis on sample *C* at a differential pressure of 17.5 MPa and butane saturation. From the least-squares fit, we estimate the variance in our estimate of E and ν.

this dependence, resulting from open cracks and compliant pores at low differential pressures. A second-order polynomial is fit to the ultrasonic traveltime data as a function of pressure (dashed and solid lines in Figure 5), and we obtain the variance of the random error. We then compute the error of our estimated traveltimes.

The ends of our samples are machine flattened; when the length is measured repeatedly, no significant variability is observed, so we consider the length is error free. We also assume there is no error in the differential-pressure measurements. Therefore, we propagate only the estimated traveltime error into the P- and S-wave velocity. Now, to estimate the bulk and shear moduli, we need the rock density, which depends on porosity, grain density, and fluid density. We assume that the variance of the rock density is 0.5% (which is in the lower end of errors reported in core measurements). In this way, we propagate the error in S-wave velocity and rock density into the shear modulus; then we propagate the P-wave velocity, rock density, and shear-modulus variance into the bulk modulus. On average, one standard deviation of the estimated P- and S-wave traveltimes is small ($\hat{\sigma}_t = 0.06\ \eta$s). Still, a small error in the rock density (0.5%) significantly affects the error of the bulk- and shear-moduli estimates ($\hat{\sigma}_K = 2.4$ GPa and $\hat{\sigma}_\mu = 0.8$ GPa) compared to the errors for data from the stress-strain experiment.

Frequency averaging

Because we acquired data for many frequencies, for the purposes of comparison we limit our analysis to 100 Hz, which is representative of seismic frequency. This distinct frequency value, together with the ultrasonic data, gives us estimates of dispersion for the bulk and shear moduli. To estimate the rock moduli at 100 Hz, we apply a least-squares fit to the logarithm (base 10) of frequency versus Poisson's ratio and Young's modulus for each sample and saturation and pick data at 100 Hz. Figure 2 is an example relating the estimated (solid line) and measured (symbols) bulk moduli for sample *H*. This procedure is only for smoothing purposes. We do not claim that this linearity fully describes the dispersion relation.

VARIATIONS IN SHEAR MODULUS

Fluids have a shear modulus of zero, so we expect the dry- or fluid-saturated rock shear modulus to be constant (true for many rocks that are isotropic and homogeneous). Together with the assumption in Gassmann's theory that pore fluids do not chemically alter the mechanical properties of a rock, Gassmann's theory predicts that the shear modulus will remain constant under different saturations. Thus, a measure of the shear modulus is one way to validate Gassmann's theory.

However, our carbonate samples show rock shear modulus changes, from dry to brine saturation, of up to 20%. Several laboratory studies have also reported shear-modulus changes between 5% and 20% from dry to water or brine saturation in carbonates (Vo-Thanh, 1995; Assefa et al., 2003; Baechle et al., 2005; Røgen et al., 2005; Sharma et al., 2006). The shear modulus of the rock is also sensitive to small amounts of moisture or partial saturation of water (Clark et al., 1984).

Rock weakening resulting from fluids has also been observed in field data. Water, weakening the rock frame in carbonates, is invoked as a primary factor controlling subsidence of the Ekofisk field. Sylte et al. (1999) show that compaction of Ekofisk chalks occurs only in chalks that are being waterflooded. High-porosity chalks that have original water content (prewaterflooding) are not compacting and behave elastically throughout the lifetime of the field. They conclude that the injected water weakens invaded chalks, resulting in compaction and porosity loss. In their study, they compare observation to geomechanical models but do not give the physicochemical mechanisms that could be producing this weakening.

Khazanehdari and Sothcott (2003) compiled rock-fluid interactions that explain the rock shear-modulus (μ) variability with fluids. They define rock weakening when $\mu_{sat} < \mu_{dry}$, and strengthening for $\mu_{sat} > \mu_{dry}$. Cardona et al. (2001), based on work from Brown and Korringa (1975), show that for an anisotropic rock, the vertically propagating shear waves are sensitive to the compressibility of the saturating fluid. However, our rocks are largely isotropic at the core scale, although they might be anisotropic at field scale. Therefore, in our work, we will focus on the rock-fluid interactions responsible for rock shear-modulus changes.

Data examples of shear-modulus sensitivity to fluids and possible explanations

Figure 6 shows the rock shear modulus for sample *C* at seismic and ultrasonic frequencies when dry and brine saturated. Error bars represent one standard deviation of the shear modulus. Two main observations are to be drawn from Figure 6. First, the rock shear modulus can either weaken or strengthen upon brine fluid saturation compared to the dry rock. At 100 Hz, we observe shear modulus weakening from dry to wet; while for 0.8 MHz data, the shear modulus strengthens when brine fills the pore space. This implies that more than one rock-fluid mechanism is active.

Second, for the 100-Hz frequency measurements, the shear modulus weakens more for low than for high differential pressures. Our measurements are performed going from high to low differential pressures (unloading cycle). After the experiment with brine saturation reached 3.5 MPa, we increased the differential pressure again for three pressure stages (circles in Figure 6). Observe that the rock shear-modulus sensitivity to brine saturation for both 100 Hz and 0.8 MHz is repeatable; thus, the shear-modulus weakening is not affected by hysteresis. This reversible weakening or strengthening of the frame is likely associated with the opening and closing of compliant pores or cracks. Some of these cracks are intrinsic to the rock,

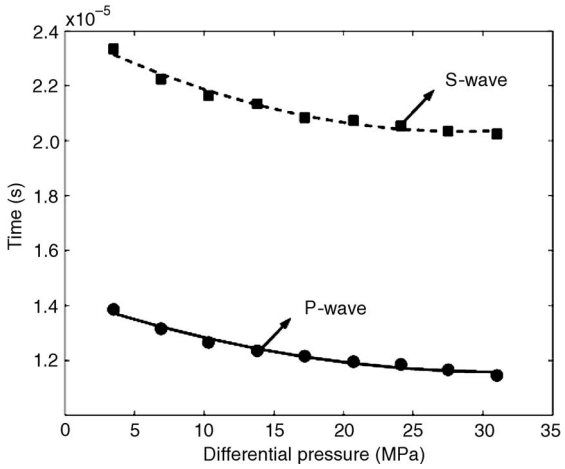

Figure 5. Second-order polynomial fit to ultrasonic traveltimes as a function of differential pressure for sample *D* under butane saturation.

while others might have been induced while drilling or coring. Other samples with significant shear-modulus weakening show similar pressure dependence to sample *C*.

Figure 7 compares the dry- and brine-saturated rock shear modulus for all samples for 100 Hz at 3.5 and at 31 MPa differential pressure. The solid line indicates equal dry- and brine-saturated shear modulus. Most samples have a rock shear modulus around 10 MPa. This cluster of data corresponds to samples with high porosity (24%–35%), while the low-porosity samples have a shear modulus larger than 15 MPa. The error bars of the shear modulus (one standard deviation) are within the size of the marker. Observe that at low differential pressures (3.5 MPa), all samples show shear modulus weakening; while at higher pressures (31 MPa), shear modulus weakening is still present but less significantly than for low pressure (see also Figure 6).

Most samples at ultrasonic frequency and at both 3.5 and 31 MPa differential pressure show neither weakening nor strengthening of the rock shear modulus within the data uncertainty (Figure 8). Weakening is observed in samples *B* and *D* but less than for seismic frequency (Figure 7).

When we compare Figures 7 and 8, the shear modulus for brine-saturated rock at ultrasonic frequency is greater than for seismic frequency. This comparative strengthening could describe modulus dispersion as a result, for example, of global- and squirt-fluid flow in the pore space. However, for samples *B* and *D*, the chemical softening of the rock could be dominating over the modulus dispersion. Alternatively, our ultrasonic-wave velocity represents the fastest path (stiffest area in the rock). If the chemical weakening is occurring in an isolated area of the sample, the stress-strain experiment measures the effective rock deformation (frame softening), while the ultrasonic wave will avoid this area and propagate in the unperturbed rock.

We also saturated the carbonate rocks with butane, a highly compressible, light hydrocarbon (in liquid phase at our elevated pore pressures). The sensitivity of the rock shear modulus to this fluid is much less than for brine (Figure 9).

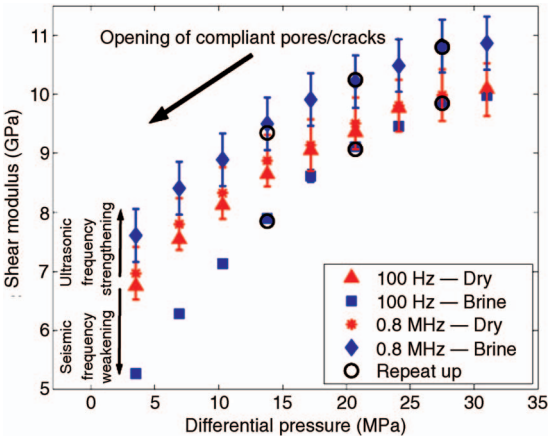

Figure 6. Sample *C*, showing shear-modulus weakening and strengthening at seismic and ultrasonic frequencies, respectively. Measurements are performed from high to low differential pressures. Circles represent repeated differential pressures going from low to high differential pressures after the initial unloading cycle was finalized. As we decrease the differential pressure, more compliant pores and cracks open. Error bars are one standard deviation (one σ for seismic frequency data is contained in the size of the symbol).

We can now examine what are the possible weakening and strengthening mechanisms acting on our carbonate rocks based on the work of Khazanehdari and Sothcott (2003). They compiled several mechanisms that can cause the shear modulus to either weaken or strengthen when a fluid contacts the solid matrix.

Pores and microfractures create surface area in a rock. Surface-energy reduction (Murphy, 1982; Murphy et al., 1986; Tutuncu and Sharma, 1992) and subcritical crack-growth mechanisms (Atkinson, 1984) relate to the amount of surface area in a porous rock. Compliant pores and microfractures are observed in our samples from thin sections. We also know, from the modulus as a function of differential pressure, that compliant pores and microfractures open, increasing the surface area as the differential pressure decreases (Figure 6). For our samples, open low-aspect-ratio pores might exhibit growth as well as breakage of solid bounds because of interaction with brine. These two mechanisms, acting on our carbonate samples, are consistent with the fact that a nonpolar fluid such as butane, saturating the rock, does not show significant shear-modulus variation (Figure 9). Another rock-fluid mechanism such as viscous coupling (Bourbié et al., 1987) is probably not the cause of shear-modulus variability in carbonates because the sensitivity to brine is large, but it is not sig-

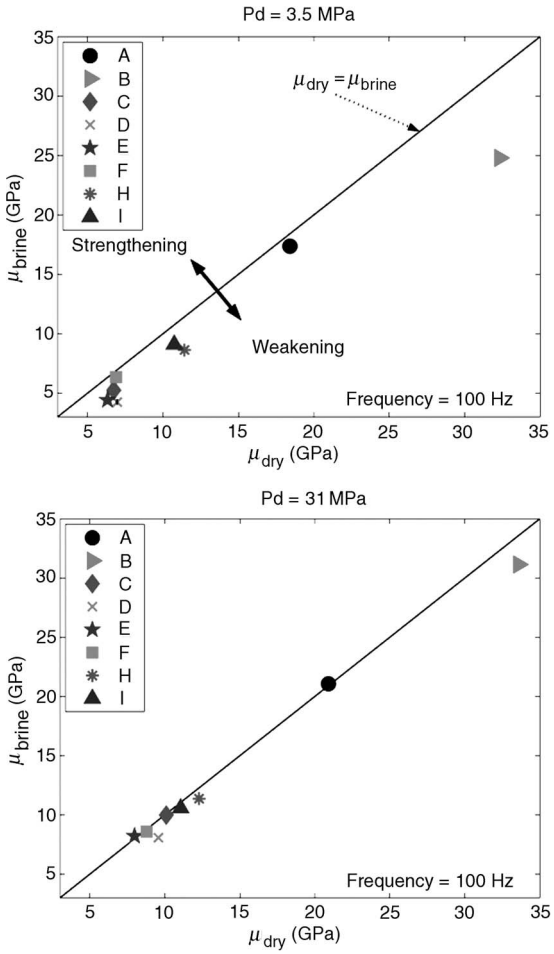

Figure 7. Shear-modulus weakening in carbonate samples resulting from dry to brine saturation at seismic frequency (100 Hz) for differential pressures of 3.5 and 31 MPa. Error bars, representing one standard deviation, are within the size of the marker for most samples.

nificant for liquid butane, with both fluids having similar and low viscosities (0.2 cp for liquid butane and 1 cp for brine). Dissolution of carbonate minerals could also be occurring. Dissolution of calcite and dolomite minerals depends on the pH of the fluid, temperature, and the reaction order of the cations (Ca, Mg, Ba), which control the dissolution rate of carbonate minerals (Chou et al., 1989).

By acquiring data at seismic and ultrasonic frequencies, we observe evidence of at least three mechanisms for which the shear modulus weakens (surface-energy reduction and crack growth) or strengthens (modulus dispersion). Changes in shear modulus could be observed from seismic time-lapse data, especially in the presence of compliant pores and polar fluids such as water. When injecting water into an oil reservoir, the nature of this polar fluid, its viscosity, pressure, temperature, etc., will likely interact with the rock solid phases, weakening or strengthening the shear modulus (and in some cases the bulk modulus) compared to the original fluid saturation.

Also, when logging data are available in a field, the analysis has to consider that modulus dispersion can be significant and should be taken with care if compared to seismic data. Log data will fall in between our measured frequency ranges ($\sim$10 KHz). Having knowledge of the characteristic frequency f_c might help the interpretation of log data. The f_c separates the behavior for relaxed and unrelaxed fluids. If $f_{\log} < f_c$ and we have compliant pores, we could observe weakening of the shear modulus upon water saturation. On the other hand, if the $f_{\log} > f_c$, strengthening of the shear modulus might be observed. Sharma et al. (2006) compiled results for the shear modulus change from dry to water saturation from several authors. In this study, the shear modulus strengthens at ultrasonic frequencies and weakens for sonic frequencies ($\sim$10 KHz) for data by Lucet (1989). This observation is in agreement with our observations on shear modulus change from seismic to ultrasonic frequencies.

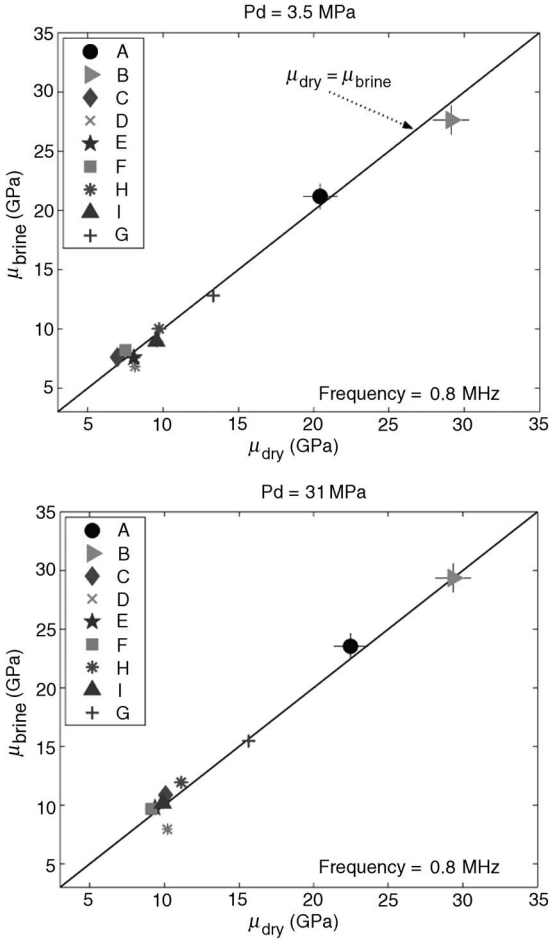

Figure 8. Carbonate samples showing that the shear modulus remains almost constant from dry to brine saturation at ultrasonic frequency for differential pressures of 3.5 and 31 MPa. Error bars, representing one standard deviation, are within the size of the marker for most samples.

GASSMANN'S FLUID SUBSTITUTION

In this section we compare and analyze the computed saturated bulk modulus, using Gassmann's theory, to the measured rock bulk modulus. Our experimental setting for seismic-frequency data acquisition lets us acquire data when the fluid is at equilibrium. The pore pressure is held constant; thus, the fluid modulus is 0.5 GPa for butane and 3.4 GPa for brine.

Figure 10 compares the bulk modulus, calculated using the Gassmann theory, to the measured modulus for butane-saturated carbonates at frequencies of 100 Hz and 0.8 MHz and at a differential pres-

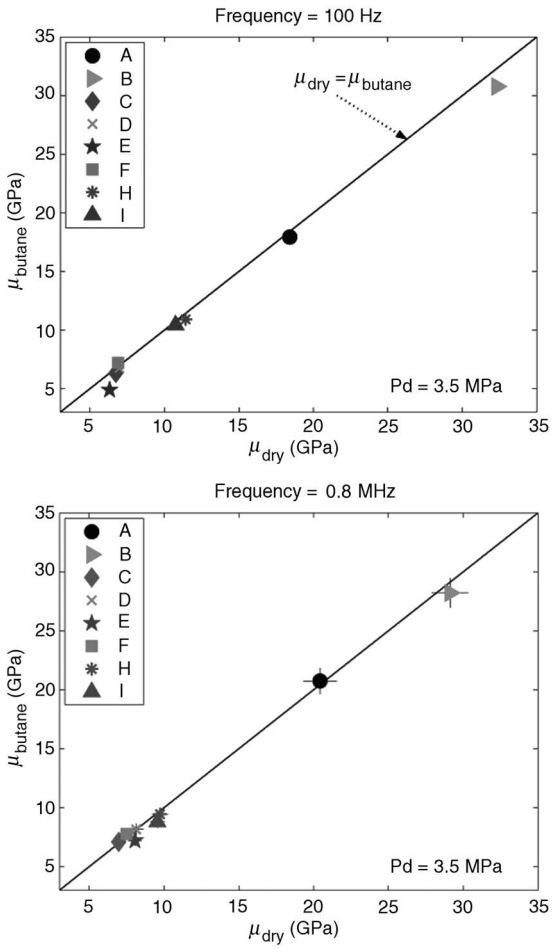

Figure 9. Carbonate samples showing little shear-modulus weakening and strengthening resulting from dry to butane saturation compared to the dry-brine saturation case. Both plots are at a differential pressure of 3.5 MPa for seismic and ultrasonic frequencies. Error bars, representing one standard deviation, are within the marker size for most samples.

sure of 31 MPa. The solid line represents the case where the butane-substituted modulus, predicted by Gassmann's theory, and the measured bulk modulus are equal. Error bars represent one standard deviation for the bulk modulus. Gassmann's theory is correctly predicting the observed butane-saturated modulus for our carbonate samples, partly because the influence of butane on the rock bulk modulus is not large. Butane is a highly compressible fluid; thus, the fluid influence on rock compressibility is not significantly different from the dry rock (see Figure 2).

For brine saturation, Gassmann-calculated and measured bulk modulus — at 100 Hz and 0.8 MHz and at differential pressures of 3.5 and 31 MPa — are compared in Figures 11 and 12, respectively. The solid line represents the case where the fluid-substituted and measured moduli are equal. Error bars represent one standard deviation for the bulk modulus. Observe that some samples match the predictions well while others do not.

In Figure 11, at a frequency of 100 Hz, none of the predictions fit the observed bulk modulus within the associate uncertainty; while at 0.8 MHz, for the same differential pressure of 3.5 MPa, the fit to the predicted bulk modulus is better. At low differential pressure and at 100 Hz, the bulk moduli for all of the samples but *F* are overpredicted by Gassmann's theory. We observe shear-modulus weakening for all samples (and the least for sample *F*, Figure 7); therefore, if the rock frame has weakened in the presence of brine, so could the bulk modulus, a factor not accounted for in Gassmann's theory. Therefore, the overprediction of the bulk modulus by Gassmann's theory at low differential pressure is probably because the rock frame has been altered (softened).

The bulk modulus is underpredicted for 100 Hz, yet it is well predicted at 0.8 MHz (Figure 11). This is largely a result of modulus dispersion. Remember that Gassmann's theory estimates the saturated modulus for low frequencies. Gassmann's theory uses the bulk modulus of the dry rock, which is not dispersive, to predict the saturated rock modulus. However, modulus dispersion exists in most of our brine-saturated carbonates (see Figure 2). This bulk modulus dispersion is evidenced in the shifting of data points in Figure 11 as the frequency increases from 100 Hz to 0.8 MHz. The bulk-modulus shift occurs parallel to the *x*-axis (measured saturated bulk modulus). This bulk-modulus dispersion at ultrasonic frequency can lead to errors when comparing ultrasonic to seismic data. Thus, a better fit at ultrasonic frequency might be somewhat of a paradox on Gassmann's theory applicability for carbonates.

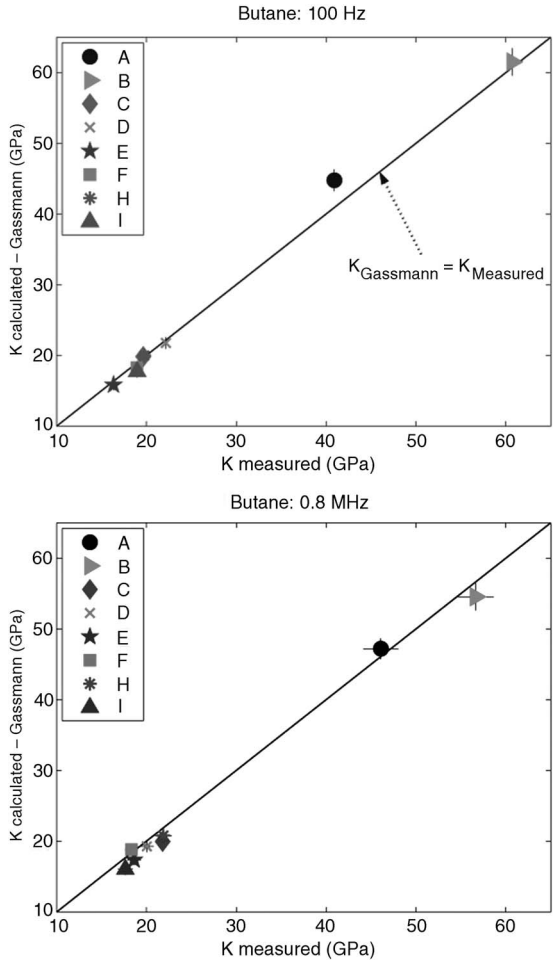

Figure 10. Butane-saturated bulk moduli measured and estimated with Gassmann's theory for 100 Hz and 0.8 MHz at 31 MPa differential pressure. Solid line represents equal measured and estimated bulk moduli. Error bars are one standard deviation of the bulk modulus.

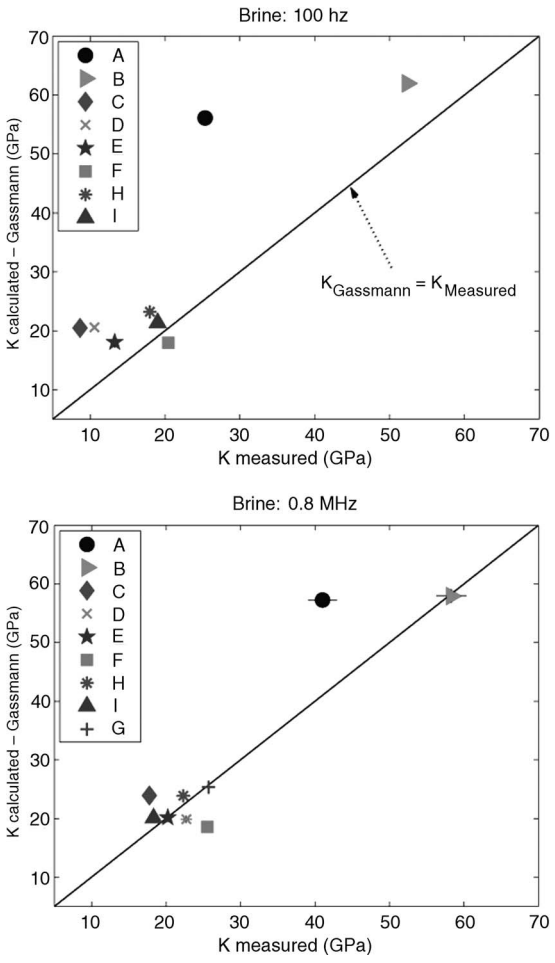

Figure 11. Brine-saturated bulk moduli measured and estimated with Gassmann's theory for 100 Hz and 0.8 MHz at 3.5 MPa differential pressure. Solid line represents equal measured and estimated bulk moduli. Error bars are one standard deviation of the bulk modulus.

At a differential pressure of 31 MPa (Figure 12), the 100-Hz data show that the bulk modulus of four brine-saturated carbonates (*B*, *E*, *I*, and *H*) is predicted well by Gassmann's theory. The bulk moduli for samples *A* and *C* are largely overpredicted by Gassmann's theory. Samples *A* and *C* have the highest content of noncalcareous minerals, especially clay. We ignore that softening of clays is a possible mechanism for elastic moduli weakening for most of our samples. However, that $K_{measured}$ is significantly less than $K_{Gassmann}$ for samples *A* and *C* is possibly related to frame (clay) weakening in the presence of brine.

We focus now on data at 100 Hz, where frequencies are low enough that we expect the fluid-pressure gradients are zero, as Gassmann's theory requires. Still, at high differential pressure, we observe that some samples are well predicted by Gassmann's theory, while others are not. So where can this difference come from? On one hand, we have observed rock shear-modulus sensitivity to brine saturation. On the other hand, for low differential pressures, we expect to have open compliant pores or cracks. Gassmann's equations are derived without assuming any specific pore geometry and can be applied to any pore type as long as the assumptions for Gassmann's theory are satisfied, i.e., pore pressure is in equilibrium. The mismatch between observed and Gassmann-predicted bulk modulus could relate to differences in pore type creating pressure gradients or chemical reactions that violate Gassmann's assumptions. Therefore, samples yielding better predictions by Gassmann's theory might be explained through the dependence of bulk modulus with differential pressure. Figure 13 plots the bulk modulus of brine-saturated carbonates as a function of differential pressure. The anomalous behavior of sample *D* at 20.7 MPa is from a small gas leak into the rock when the sample was saturated with brine. This dramatically lowered the bulk modulus of sample *D* at low frequencies for pressures lower than 20.7 MPa. In Figure 13, we observe a consistent linear behavior of the bulk modulus with differential pressure from the Hertz-Mindlin model: $K = mP^{1/3}$ (Mavko et al., 1998), where the slope of the linear trends are different for different rocks. Higher slopes mean larger dependence on differential pressure, indicating the existence of compliant pores or microcracks. Table 2 compares Gassmann's predictability, shear-modulus weakening, mineralogy, and pressure effect on all samples at 100 Hz. Gassmann's predictability and shear-modulus weakening are reported for the highest differential pressure reached at 31 MPa. The pressure effect is measured by the slope of the linear dependence of the bulk modulus (Figure 13).

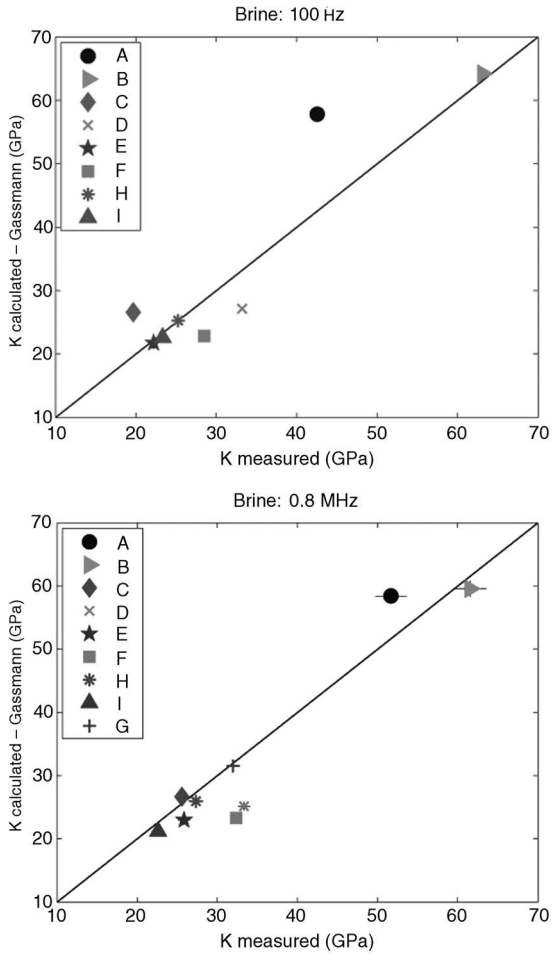

Figure 12. Brine-saturated bulk moduli measured and estimated with Gassmann's theory for 100 Hz and 0.8 MHz at 31 MPa differential pressure. Solid line represents equal measured and estimated bulk moduli. Error bars are one standard deviation of the bulk modulus.

There seems to be no correlation between shear-modulus weakening and the observed match between measured and computed bulk moduli for brine-saturated carbonates at high differential pressure (Table 2). For example, both samples *B* and *D* show significant shear-modulus weakening at 31 MPa differential pressure; still, sample *B* is well predicted by Gassmann's theory, but sample *D* is not. It might seem confusing that although Gassmann's assumption that the rock frame stays unaltered by the fluid is violated for some samples, the measured brine-saturated bulk modulus is well predicted by Gassmann's theory for these samples. A likely reason for this is because the increase in bulk modulus, in absolute percent from dry to brine saturation (35% in average), is more significant than the shear modulus weakening in absolute percent (6% in average).

Examining the pressure dependence, the saturated bulk modulus for samples with lower slopes (*B*, *E*, *H*, and *I*) is well predicted by Gassmann's theory. Low slopes mean the sample has less-compliant pores or cracks. Samples *A*, *C*, and *D* have high slopes, and Gassmann's theory is not predicting the observed saturated bulk modu-

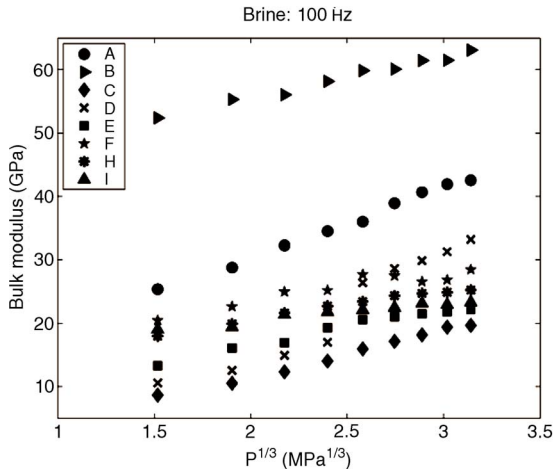

Figure 13. Bulk modulus for carbonates with brine saturation as a function of differential pressure ($P^{1/3}$) for 100 Hz.

Table 2. Gassmann's theory applicability correlated with shear-modulus weakening and bulk-modulus dependence with pressure (slopes of Figure 13). Gassmann and shear-modulus analysis corresponds to 100 Hz at a differential pressure of 31 MPa. The X means the statement is true. Dominant mineralogy: C = calcite, D = dolomite. Note correspondence of good Gassmann's theory fit with low-pressure dependence *m*.

Samples	A	B	C	D	E	F	H	I
Gassmann's theory fits		X			X		X	X
Shear-modulus weakening		X		X			X	
Bulk modulus vs. pressure (*m*)	11.8	5.6	7.9	11.2	5.2	5.4	4.5	3.2
Mineralogy	C	D	C	C	C	C	D	D

lus. Sample *F* has an intermediate slope, but the saturated bulk modulus is not well predicted by Gassmann's theory. For sample *F*, the bulk modulus as a function of pressure is less smooth than for other samples, leading to a higher variance in the slope calculation. As previously mentioned, our experimental setup could not quite reach the differential pressure of the reservoir at 34.5 MPa. This could result in some compliant pores still being open at these pressures. From this, we conclude that open compliant pores are a possible factor affecting the mismatch between observed and predicted bulk modulus. Samples *B*, *H*, and *I* are dolomites, but we do not have enough statistical data to make correlations with rock-grain density. Nevertheless, these dolomite samples have high porosity and permeability, probably satisfying Gassmann's assumption on pore connectivity and fluid distribution in the porous space.

From our observations, carbonates with round pores, vugs, or micritic textures are well predicted by Gassmann's theory for low frequencies. Even at reservoir pressures, open compliant pores or cracks might be present at reservoir in-situ conditions. In this case, an anisotropic fluid-substitution theory, such as that of Brown and Korringa (1975), is perhaps more appropriate. However, knowledge of the anisotropic symmetry, with all of the stiffness coefficients of the rock and the pore-space compressibility, are required for this theory. Using additional parameters might allow one to fit the data better, but these estimated parameters could not be realistic or representative of the rock.

CONCLUSIONS

We present data over a large range of frequencies and under varying saturation and pressure conditions to investigate the applicability of Gassmann's theory for our carbonate data set. We observe that the rock shear modulus is sensitive to brine saturation, especially at seismic frequencies. Weakening of the solid matrix occurs possibly due to surface energy loss and/or subcritical crack growth in compliant pores, mostly at low differential pressures. These mechanisms violate an assumption of Gassmann's theory that the fluid does not influence the solid matrix of the rock. However, we find no positive correlation between the rock shear-modulus weakening and the failure of Gassmann's theory to predict the saturated bulk modulus at seismic frequencies and high differential pressures. We do find that the brine-saturated bulk modulus for carbonates with small differential pressure dependence (round pores or vugs) is well predicted by Gassmann at seismic frequencies and high differential pressures, while for carbonates strongly influenced by pressure (compliant pores or microcracks), Gassmann's theory does not match the observations. Therefore, knowledge of the reservoir pore-space geometry can aid in understanding and applying Gassmann's theory.

Predicting the saturated bulk modulus at ultrasonic frequencies violates Gassmann's low-frequency assumption. Nevertheless, we test our carbonate samples at ultrasonic frequencies to show the role of modulus dispersion. For some of our samples, the measured and Gassmann-calculated bulk moduli at ultrasonic frequencies show better agreement compared to seismic frequencies. This match is apparent, resulting from bulk modulus dispersion, which we observe in our carbonates when saturated with brine. We also observe shear-modulus dispersion. Little change from dry to brine saturation is present in the rock shear modulus at ultrasonic frequencies, but this modulus is always higher than the shear modulus obtained at seismic frequencies. This increase could be a result of dispersion or a preferential propagation path, which avoids altered (weakened) sections in the saturated rocks. Although our conclusions are based on samples with different texture and mineralogy, we must be careful to generalize these results to all carbonate rocks.

Our observations are applicable particularly to the analysis of time-lapse data. Ultrasonic laboratory data is used in some cases to calibrate time-lapse seismic reflection data. We should be aware that bulk modulus in carbonate rocks can have significant dispersion affecting the applicability of Gassmann's fluid-substitution theory at ultrasonic frequencies (and maybe at log frequencies). Also, when water or brine replaces a nonpolar fluid such as oil, shear-modulus weakening can be observed in the field. Brine of different salinity and temperature injected in an aquifer to enhance production might change the solid frame, causing variation in the moduli of the rocks.

ACKNOWLEDGMENTS

We would like to thank Statoil for providing the cores and useful discussions. We also thank De-Hua Han for measuring sample *G* at ultrasonic frequencies and K/T GeoServices Inc. for the XRD analysis. We would like to thank Kasper van Wijk, as well as Ronny Hofmann, Manika Prasad, Martin Landrø, Luis Tenorio, John Scales, Thomas Davis, and Dave Hale, for their feedback and discussions. We also thank the support of all of the members of the Fluid and DHI Consortia.

REFERENCES

Anselmetti, F. S., and G. P. Eberli, 1993, Controls on sonic velocity in carbonates: Pure and Applied Geophysics, **141**, 287–323.
Assefa, S., C. McCann, and J. Sothcott, 2003, Velocities of compressional and shear waves in limestones: Geophysical Prospecting, **51**, 11–13.
Atkinson, B. K., 1984, Subcritical crack growth in geological materials: Journal of Geophysical Research, **89**, 4077–4114.
Baechle, G. T., R. J. Weger, G. P. Eberli, J. L. Massaferro, and Y.-F. Sun, 2005, Changes of shear moduli in carbonate rocks: Implications for Gassmann applicability: The Leading Edge, **24**, 507–510.
Batzle, M. L., D.-H. Han, and R. Hofmann, 2006, Fluid mobility and frequency-dependent seismic velocity: Direct measurements: Geophysics, **71**, N1–N9.
Berryman, J. G., 1999, Origin of Gassmann's equations: Geophysics, **64**, 1627–1629.
Biot, M. A., 1956, Theory of propagation of elastic waves in a fluid-saturated porous solid. I. Low-frequency range: Journal of the Acoustical Society of America, **28**, 168–178.
Birch, F., 1960, The velocity of compressional waves in rocks to 10 kilobars, Part 1: Journal of Geophysical Research, **65**, 1083–1102.

Bourbié, T., O. Coussy, and B. Zinszner, 1987, Acoustics of porous media: Gulf Publishing Company.
Brown, R., and J. Korringa, 1975, On the dependence of the elastic properties of a porous rock on the compressibility of the pore fluid: Geophysics, **40**, 608–616.
Cardona, R., M. Batzle, and T. L. Davis, 2001, Shear wave velocity dependence on fluid saturation: 71st Annual International Meeting, SEG, Expanded Abstracts, 1712–1715.
Chou, L., R. M. Garrels, and R. Wollast, 1989, Comparative study of the kinetics and mechanisms of dissolution of carbonate minerals: Chemical Geology, **78**, 269–282.
Clark, V. A., B. R. Tittmann, and T. W. Spencer, 1984, Rock lithology and porosity determination from shear and compressional wave velocity: Geophysics, **49**, 1188–1195.
Domenico, S. N., 1984, Rock lithology and porosity determination from shear and compressional wave velocity: Geophysics, **49**, 1188–1195.
Dutta, N. C., and H. Ode, 1979, Attenuation and dispersion of compressional waves in fluid-filled porous rocks with partial gas saturation (White model): Part II: Results: Geophysics, **44**, 1789–1805.
Gassmann, F., 1951, Uber die elastizität poröser medien: Vierteljahrsschrift der Naturforschenden Gesellschaft in Zürich, **96**, 23.
Han, D.-H., 2004, Velocity in carbonate rocks: Fluids and DHI Consortia Sponsor Meeting, Technical Report.
Hudson, J. A., 1981, Wave speeds and attenuation of elastic waves in material containing cracks: Geophysical Journal of the Royal Astronomical Society, **64**, 133–150.
Khazanehdari, J., and J. Sothcott, 2003, Variation in dynamic elastic shear modulus of sandstone upon fluid saturation and substitution: Geophysics, **68**, 472–481.
Kuster, G. T., and M. N. Toksoz, 1974, Velocity and attenuation of seismic waves in two-phase media: Part I. Theoretical formulations: Geophysics, **39**, 587–606.
Lucet, N., 1989, Vitesse et attenuation des ondes elastiques soniques et ultrasoniques dans les roches sous pression de confinement: Ph.D. thesis, University of Paris.
Marion, D., and D. Jizba, 1997, Acoustic properties of carbonate rocks: Use in quantitative interpretation of sonic and seismic measurements *in* I. Palaz and K. J. Marfurt, eds., Carbonate seismology: SEG, 75–93.
Mavko, G., and D. Jizba, 1991, Estimating grain-scale fluid defects on velocity dispersion in rocks: Geophysics, **56**, 1940–1949.
Mavko, G., T. Mukerji, and J. Dvorkin, 1998, The rock physics handbook: Cambridge Univ. Press.
Moore, C. H., 2001, Carbonate reservoirs: Porosity evolution and diagenesis in a sequence stratigraphic framework: Developments in sedimentology: Elsevier Science Publ. Co., Inc.
Murphy, W. F., 1982, Effects of partial water saturation on attenuation in Massilon sandstone and Vycor porous glass: Journal of the Acoustical Society of America, **71**, 1458–1468.
Murphy, W. F., K. W. Winkler, and R. L. Kleinberg, 1986, Acoustics relaxation in sedimentary rocks: Dependence on grain contacts and fluid saturation: Geophysics, **51**, 757–766.
O'Connell, R. J., and B. Budiansky, 1974, Stress-induced velocities in dry and saturated cracked solids: Journal of Geophysical Research, **79**, 4626–4627.
Røgen, B., I. L. Fabricius, P. Japsen, C. Høier, G. Mavko, and J. M. Pedersen, 2005, Ultrasonic velocities of North Sea chalk samples: Influence of porosity, fluid content and texture: Geophysical Prospecting, **53**, 481–496.
Sharma, R., M. Prasad, G. C. Katiyar, and G. Surve, 2006, In the applicability of Gassmann model in carbonates: Society of Petroleum Geophysicists Conference, India.
Spencer, J. W., 1981, Stress relaxation at low frequencies in fluid saturated rocks: Attenuation and modulus dispersion: Journal of Geophysical Research, **86**, 1803–1812.
Sylte, J. E., L. K. Thomas, D. W. Rhett, D. D. Bruning, and N. B. Nagel, 1999, Water induced compaction in the Ekofisk field: Society of Petroleum Engineers Annual Technical Conference, SPE 56426.
Tutuncu, A. N., and M. M. Sharma, 1992, The influence of fluids on grain contact stiffness and frame moduli in sedimentary rocks: Geophysics, **57**, 1571–1582.
Vo-Thanh, D., 1995, Influence of fluid chemistry on shear-wave attenuation and velocity in sedimentary rocks: Geophysical Journal International, **121**, 737–749.
Wang, Z., 1997, Seismic properties of carbonate rocks *in* I. Palaz and K. J. Marfurt, eds., Carbonate seismology: SEG, 29–52.
——–, 2000, The Gassmann equation revised: Comparing laboratory data with Gassmann's predictions *in* Z. Wang, A. Nur, and D. A. Ebrom, eds., Seismic and acoustic velocities in reservoir rocks: SEG, 8–23.
Wang, Z., W. K. Hirsche, and G. Sedgwick, 1991, Seismic monitoring of water floods? A petrophysical study: Geophysics, **56**, 1614–1623.
White, J. E., 1975, Computed seismic speeds and attenuation in rocks with partial gas saturation: Geophysics, **40**, 224–232.